Removal of aqueous rare earth elements (REEs) using nano-iron based materials

Dataset *in* Journal of Industrial and Engineering Chemistry · May 2013

DOI: 10.1016/j.jiec.2012.11.005

3 authors, including:

Semira Ünal Yeşiller
Izmir Institute of Technology
7 PUBLICATIONS **58** CITATIONS
SEE PROFILE

Talal Shahwan
Birzeit University
54 PUBLICATIONS **1,293** CITATIONS
SEE PROFILE

Journal of Industrial and Engineering Chemistry 19 (2013) 898–907

Contents lists available at SciVerse ScienceDirect

Journal of Industrial and Engineering Chemistry

journal homepage: www.elsevier.com/locate/jiec

Removal of aqueous rare earth elements (REEs) using nano-iron based materials

S. Unal Yesiller [a], A.E. Eroğlu [a], T. Shahwan [b,*]

[a] Department of Chemistry, İzmir Institute of Technology, Urla 35430, İzmir, Turkey
[b] Department of Chemistry, Birzeit University, Ramallah, West Bank, Palestine

ARTICLE INFO

Article history:
Received 23 June 2012
Accepted 4 November 2012
Available online 10 November 2012

Keywords:
Rare earth elements
nZVI
Iron oxide
Alumina
Al-nZVI
Uptake

ABSTRACT

The uptake of REEs was investigated using nano-zero valent iron (nZVI) and alumina-supported nZVI (Al-nZVI). The results indicated fast uptake, with saturation approached within 10 min of contact between solutions and solids. Upon using nZVI, the uptake of REEs seemed to be quantitative over the studied range of concentration; 1.0–100.0 mg L^{-1}. When Al-nZVI was used, complete removal was achieved within the range of 1.0–10.0 mg L^{-1}. The solids demonstrated stable performance beyond pH of 2.0, up to neutral pH conditions. Fractionation of REEs on Al-nZVI was observed. The REE ions seem to be fixed to oxide and oxyhydroxide surface groups.

1. Introduction

Rare earth elements are not quite rare as the name suggests. These elements are relatively plentiful in the earth crust, with many reserves in about 34 countries [1]. The REE elements are being widely used in industry due to their metallurgical, optical, and electronic properties. This includes mature markets such as catalysts, glassmaking, lighting, and metallurgy, and new high-growth markets such as battery alloys, ceramics, and permanent magnets [2]. They are also reported to be used as diagnosis reagents of magnetic resonance imaging (MRI) in medicine and some fertilizers in agriculture [3]. Anthropogenic activities may thus end up with REE metals in the hydrosphere and eventually in the food cycle and biosystem. Therefore, the isolation of these elements from the environment is an important preventive measure against harmful exposure.

So far, various methods have been used for the separation/preconcentration or removal of trace REEs from various matrices. These include coprecipitation [4], liquid–liquid extraction [5], solid-phase extraction [6], ion-exchange [7], adsorption [8], and biosorption [9].

Although the efficiency of the above mentioned methods has been demonstrated for various applications and sample types, research and development is continuing to innovate other materials. Recently, nano-scale zero valent iron (nZVI) is emerging as a very effective counter amendment tool for various types of organic and inorganic pollutants [10–15]. The effectiveness of the material originates from the small particle size and low standard potential, easiness of preparation, in addition to being environmentally friendly, as Fe is known to possess a relatively high recommended safety limit and daily intake requirement [16], compared with other metals.

In this study, the removal of REEs is reported for the first time using nZVI produced by liquid phase reduction with sodium borohydride as a reducing agent. A composite material of nZVI and alumina (Al-nZVI) was also tried for the same purpose. The synthesis of this material and its effective performance in the removal of aqueous Cu^{2+} ions was recently reported by our group [17]. The application of alumina aimed at decreasing the well-known aggregation tendency of iron nanoparticles by providing a substrate on which individual iron nanoparticles can be dispersed. The uptake behavior of REEs on both iron materials was investigated as a function of solution pH, solution volume, contact time, initial concentration, and the reusability of the iron materials was tested. The results of the experiments presented in this study correspond to La (as a representative of the light REEs: La, Ce, Pr, and Nd), Eu (as a representative of the medium REEs: Sm, Eu, Gd, Tb, Dy, and Ho) and Yb (as a representative of the heavy REEs: Er and Yb).

The materials were characterized using scanning electron microscopy/energy dispersive X-ray spectroscopy (SEM/EDX), transmission electron microscopy (TEM), X-ray diffraction (XRD), particle size and zeta potential (ξ) measurements. The concentrations of the REEs were determined using inductively coupled plasma-mass spectrometry (ICP-MS).

* Corresponding author. Tel.: +970 2 2982146.
E-mail address: tshahwan@birzeit.edu (T. Shahwan).

1226-086X/$ – see front matter © 2012 The Korean Society of Industrial and Engineering Chemistry. Published by Elsevier B.V. All rights reserved.
http://dx.doi.org/10.1016/j.jiec.2012.11.005

2. Experimental

2.1. Reagents and materials

All reagents were of analytical grade. Ultrapure water (18 MΩ) was used throughout the study. Plastic ware was soaked in 10% (v/v) nitric acid for cleaning and rinsed three times with ultrapure water prior to use.

Standard multielement REEs stock solutions (1000 mg L^{-1}) were prepared by dissolving the appropriate amount of oxide or nitrate forms of REEs in 100.0 mL of ultrapure water in the presence of 5 mL of HNO_3 and 3 mL of HCl under moderate heating (40–50 °C) and gentle stirring on a magnetic stirrer. This stock solution was kept at 4 °C in refrigerator. The working solution of REEs was prepared fresh just before use by dilution of the stock standard solution.

$FeCl_2{\cdot}4H_2O$ was obtained from Sigma–Aldrich, ethanol and $NaBH_4$ were obtained from Merck.

The REEs concentrations were determined by an Agilent 7500 ICP-MS instrument. The operating conditions are listed in Table 1.

Table 1
The operating parameters for Agilent 7500 ICP-MS.

Forward power	1500 W
Reflected power	1 W
Coolant gas flow rate	15 L min^{-1}
Auxiliary flow rate	0.90 L min^{-1}
Sample uptake time	25 s
Integration time	100 ms
Mass of elements	^{139}La, ^{140}Ce, ^{141}Pr, ^{146}Nd, ^{147}Sm, ^{153}Eu, ^{157}Gd, ^{159}Tb, ^{163}Dy, ^{165}Ho, ^{166}Er, ^{172}Yb

2.2. Synthesis of nZVI and alumina-supported nZVI

Nanoscale Fe^0 particles were prepared in accordance with the procedure reported in our earlier studies [11] with some changes in the reagent quantities. For this purpose, 5.340 g of $FeCl_2{\cdot}4H_2O$ was dissolved in 25 mL of 4:1 ethanol/water solution and the solution was shaken for 20 min in ultrasonic shaker. Separately, 70 mL of 0.2 M $NaBH_4$ solution was prepared, and then added to the mixture using a burette, while stirring the solution using a magnetic stirrer. After the addition of the borohydride solution was completed, the mixture was mixed for additional 20 min to ensure maximum reduction of iron ions. Next, the solution was vacuum filtrated and the precipitate was washed at least three times with ethanol. Finally, it was dried in oven at 50 °C for two days. A schematic representation of the synthesis process is given in Fig. 1.

The procedure for synthesizing alumina-supported iron nanoparticles was reported in an earlier publication [17]. The reagent quantities were adjusted such that the alumina:Fe^{2+} ratio is 1:1 (m/m). For this, 5.340 g of $FeCl_2{\cdot}4H_2O$ was dissolved in 25 mL of 4:1 ethanol/water solution. Then 1.5 g of Al_2O_3 was added to the solution and shaken for 20 min in ultrasonic shaker. Separately, 70 mL of 0.2 M $NaBH_4$ solution was prepared, and was then added to the mixture using a burette, while stirring the solution using a magnetic stirrer. After the addition of the borohydride solution was completed, the mixture was mixed for additional 20 min. The solid composite was vacuum filtrated and washed at least three times with ethanol. Finally, it was dried in oven at 50 °C for 2 days.

2.3. Characterization of nZVI and alumina-supported nZVI

The solid samples were characterized using XRD, SEM/EDX, and HR-TEM. The XRD analysis of the powders was performed using a Philips X'Pert Pro diffractometer. The source consisted of Cu Kα radiation (λ = 1.54 Å). Each sample was scanned within the 2θ range of 20–70°. SEM-EDX characterization was carried out using a Philips XL-30S FEG type instrument. Prior to analysis, solid samples were sprinkled onto adhesive carbon tapes which were supported on metallic disks. The HR-TEM analysis was realized with a Tecnai F20 instrument located at the Max Planck Institute for Polymer Research-Germany. The instrument was operated at 200 kV acceleration voltage. Prior to analysis, nZVI and Al-nZVI samples were dispersed in ethanol using an ultrasonic bath and a drop of the dispersion was applied to a holey copper TEM support grid. Excess solution was blotted off using a filter paper.

The zeta potential measurements were performed using Zeta meter 3.0+ by Zeta-Meter, Inc. with molybdenum anode and platinum cathode.

2.4. Uptake studies of REEs

The uptake behavior of REEs on nZVI and Al-nZVI materials was investigated as a function of contact time, initial concentration, solution volume, and solution pH. The reusability of the iron

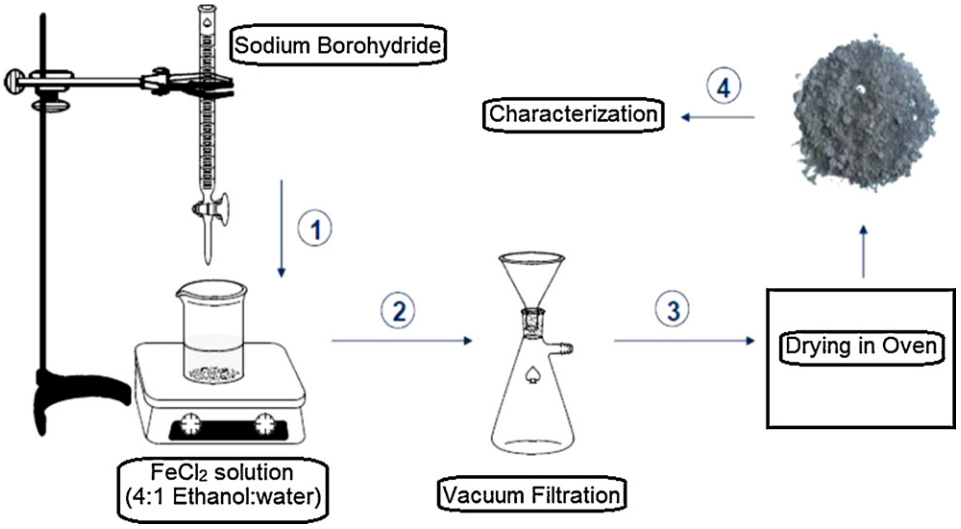

Fig. 1. Schematic representation of the synthesis of nano-iron materials by borohydride reduction.

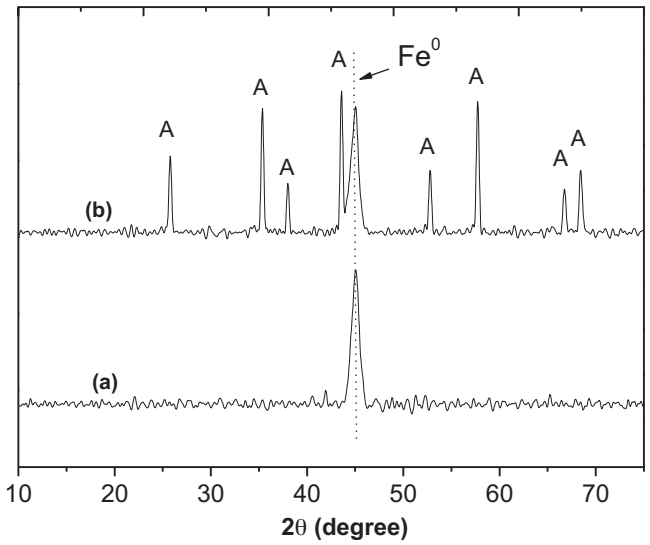

Fig. 2. XRD patterns of: (a) nZVI and (b) Al-nZVI.

materials was also tested. The uptake studies were all performed via a batch process. For the sake of comparison, parallel experiments were performed using pure alumina.

In each test, 100.0 mg samples of nZVI or Al-nZVI was added to a 10.0 mL of REEs solution at a desired concentration, and was shaken manually for 1–2 min and then placed on a lateral shaker for the desired time at room temperature.

In order to study the effect of solution pH on the uptake of REEs on nZVI and Al-nZVI, 1.0 mg L^{-1} and 100.0 mg L^{-1} multielement REE standards were prepared in different pH media varying from pH 1.0 to 8.0 in the case of 1.0 mg L^{-1}, and from pH 1.0 to 6.0 in the case of 100.0 mg L^{-1}. For the pH adjustment, dilute solutions of NH_3 (0.1–1.0 M) or HNO_3 (0.1–1.0 M) were used.

The effect of contact time was studied for time periods ranging from 5 min up to 24 h, at initial concentrations of 10.0 mg L^{-1} and 100.0 mg L^{-1} and solution pH of 5.0. The effect of initial metal concentration on the uptake percentage of REEs was investigated at the initial concentrations of 1.0, 5.0, 10.0, 50.0 and 100.0 mg L^{-1}, initial pH of 5.0, and contact time of 30 min. At the end of mixing, the solid and the liquid phases were separated by filtration and the liquid part was analyzed for REEs with ICP-MS instrument.

For testing the reusability of the iron materials, 1.0 mg L^{-1} and 50.0 mg L^{-1} multielement REEs standard solutions were prepared at a pH of 5.0. Then 100 mg of nZVI or Al-nZVI was added to 10 mL of each solution and shaken 30 min. After shaking, the mixture was centrifuged at 6000 rpm for 5 min, and the supernatant solution was filtered for ICP-MS determination. Subsequently new fresh 10 mL of REEs solutions were added on the used solid sample and the same procedure was performed. This cycle was repeated for ten successive times.

In batch sorption studies, Yellowline RS 10 (Staufen, Germany) lateral shaker was used to provide efficient mixing. The pH measurements were performed using inoLab pH720 meter.

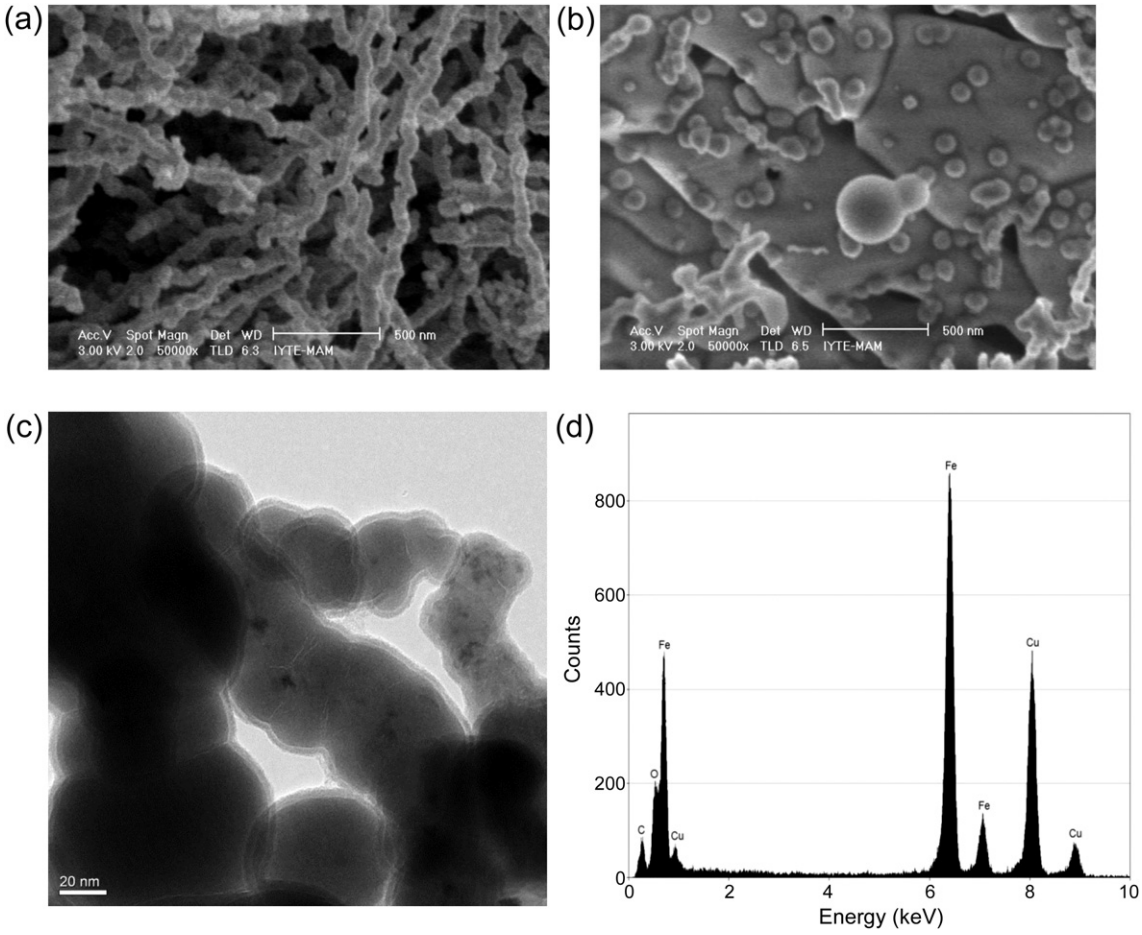

Fig. 3. (a) SEM image of nZVI, (b) SEM image of Al-nZVI, (c) TEM image of nZVI, and (d) EDX spectrum of nZVI.

Table 2
Variation of percentage uptake of various REE ions as a function of pH on alumina, Al-nZVI, and nZVI (Ci: 100.0 mg L^{-1} REEs, *V*: 10 ml, *m*: 100 mg, shaking time: 30 min).

pH	La 139			Ce 140			Pr 141		
	nZVI	Al-nZVI	Al_2O_3	nZVI	Al-nZVI	Al_2O_3	nZVI	Al-nZVI	Al_2O_3
1	90.69	49.78	27.66	96.51	63.81	28.23	97.89	70.41	28.02
3	100.00	73.15	38.55	100.00	83.74	40.51	100.00	88.09	41.05
4	100.00	66.22	40.86	100.00	77.15	42.89	100.00	82.00	43.83
5	100.00	71.27	42.89	100.00	78.74	44.69	100.00	82.19	44.90
6	100.00	75.85	41.95	100.00	76.23	43.89	100.00	79.81	44.50
pH	Nd 146			Sm 147			Eu 153		
	nZVI	Al-nZVI	Al_2O_3	nZVI	Al-nZVI	Al_2O_3	nZVI	Al-nZVI	Al_2O_3
1	98.30	73.05	27.82	99.19	81.67	28.18	99.23	82.69	28.15
3	100.00	89.88	41.58	100.00	94.86	43.16	100.00	95.36	42.72
4	100.00	84.07	44.17	100.00	91.52	45.85	100.00	92.30	45.51
5	100.00	83.70	45.03	100.00	89.21	46.07	100.00	89.78	45.94
6	100.00	81.77	45.10	100.00	88.37	46.00	100.00	89.01	46.19
pH	Gd 157			Tb 159			Dy 163		
	nZVI	Al-nZVI	Al_2O_3	nZVI	Al-nZVI	Al_2O_3	nZVI	Al-nZVI	Al_2O_3
1	98.84	78.45	31.07	99.28	83.34	28.90	99.35	83.92	29.47
3	100.00	93.46	43.38	100.00	95.98	41.07	100.00	96.36	41.38
4	100.00	88.97	46.14	100.00	93.33	43.88	100.00	94.21	43.83
5	100.00	87.12	46.87	100.00	90.43	45.08	100.00	90.82	45.40
6	100.00	85.92	46.46	100.00	89.56	44.88	100.00	90.08	44.40
pH	Ho 165			Er 166			Yb 173		
	nZVI	Al-nZVI	Al_2O_3	nZVI	Al-nZVI	Al_2O_3	nZVI	Al-nZVI	Al_2O_3
1	99.30	83.65	29.24	99.34	84.06	29.22	99.56	86.79	29.87
3	100.00	96.23	40.59	100.00	96.46	40.26	100.00	97.10	41.37
4	100.00	93.82	43.01	100.00	94.47	42.98	100.00	96.23	43.89
5	100.00	90.62	44.76	100.00	91.01	44.49	100.00	92.17	45.08
6	100.00	89.90	44.06	100.00	90.26	43.67	100.00	92.12	44.87

3. Results and discussion

3.1. Characterization results of nZVI and Al-nZVI

The XRD diagrams of the synthesized nZVI and Al-nZVI materials are given in Fig. 2. The figure shows the basic reflections of alumina in addition to that of metallic iron, which appears to be free of oxide components. Iron, in its zero-valent state, is characterized by its major reflection at $2\theta = 44.9$, in addition to other reflections at high 2θ values. Alumina appears to be free of other solid impurities up to the detection level of XRD.

The SEM analysis showed that nZVI possesses its characteristic chain-like structure as shown in Fig. 3a. The nZVI prepared in the presence of alumina retained to a large extent its chain-like morphology, but part of the nanoparticles appeared in dispersed form as shown by the SEM image in Fig. 3b. The particle size of the dispersed particles ranged between 10 and 80 nm. The identity of the dispersed nanoparticles was confirmed using multiple EDX spot analysis. The atomic ratio of Fe/Al on alumina surface ranged between 2.6 and 5.4 in the regions where nZVI was dispersed. HR-TEM images (Fig. 3c) confirmed the SEM findings, and showed that the nZVI possessed the well-known core-shell structure, with the shell being approximately 3 nm thick. Fig. 3d shows a typical EDX spectrum of nZVI. The zero point of charge (zpc) of nZVI was measured by zeta potential measurement to be 8.3, and the zpc of Al-nZVI was determined as 5.6. Further aspects about the structure of Al-nZVI can be found in our recent publication [17].

3.2. Results of the uptake experiments

The results of the experiments performed in the present study under the same conditions have shown very strong similarities in the trends of uptake of REEs by the three sorbents: nZVI, Al-nZVI, and Al_2O_3. This fact is illustrated by the sample results summarized in Table 2, which shows the variation of percentage uptake of various REE ions as a function of pH, under the given conditions. Since the amount of generated data is bulky, only the results for La (as a representative of the light REEs), Eu (as a representative of the medium REEs), and Yb (as a representative of the heavy REEs) are provided in the next sections. In the related results, the percentage uptake was calculated using the equation:

$$\%\,\text{Uptake} = \frac{C_0 - C}{C_0} \times 100\%$$

where C_0 is the initial metal concentration and C is the equilibrium concentration in the solution.

3.2.1. Effect of pH on uptake

The effect of solution pH on the uptake of REEs on the nZVI and Al-nZVI is shown in Fig. 4 at the initial concentrations of 1.0 mg L^{-1} and 100.0 mg L^{-1}. For the sake of comparison, a parallel set was conducted using alumina, and the corresponding data are contained also in Fig. 4. At the initial concentration of 1.0 mg L^{-1}, both of nZVI and Al-nZVI demonstrated almost complete removal of REEs at all the studied initial pH values. Alumina also exhibited a high uptake potential for pH values larger than 3.0. However, the differences in uptake capacity between the three materials becomes more distinct at the REEs initial concentration of 100.0 mg L^{-1}. At this concentration, the pH range was kept below 7.0 in order to avoid any bulk precipitation of REE hydroxides. It can be seen from Fig. 4(d–f) that pure nZVI showed the highest capacity at all initial pH value, and beyond pH of 2.0 the uptake seems to be complete. On the contrary, alumina

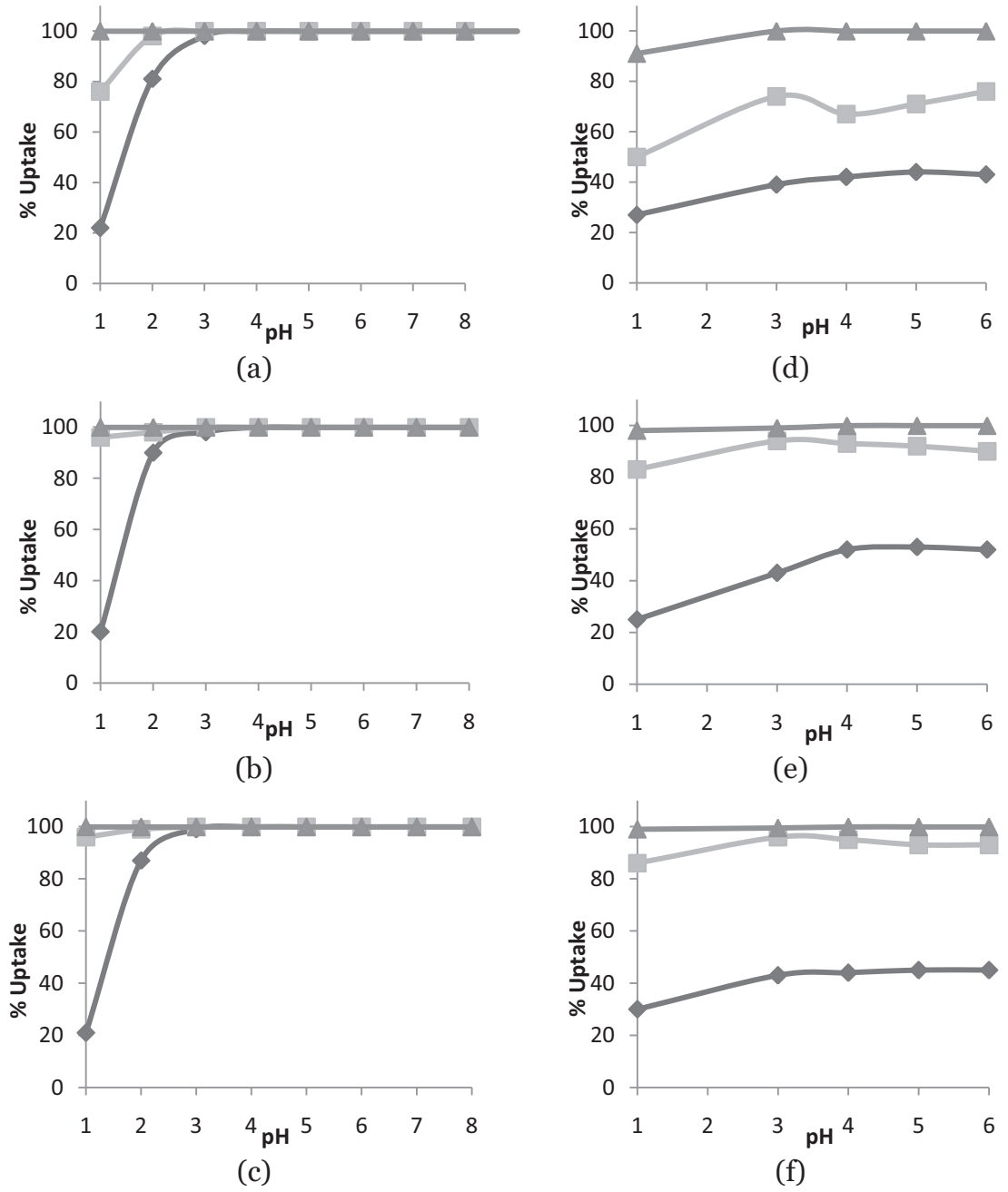

Fig. 4. Variation of percentage uptake with pH at initial concentration of 1.0 mg L^{-1} of: (a) La (III), (b) Eu(III), (c) Yb(III), and at initial concentration of 100.0 mg L^{-1} of: (d) La (III), (e) Eu(III), and (f) Yb(III). *m*: 100 mg; *V*: 10 mL; shaking time: 30 min. ◆: alumina; ■: Al-nZVI; ▲: nZVI.

demonstrated the lowest capacity (maximum value of 45–50%), with its percentage uptake of REEs increasing gradually with pH. The incorporation of nZVI with alumina enhanced the uptake capacity of the mineral significantly as reflected by the extent of uptake of Al-nZVI. Fig. 4 shows that, at low REE concentration, there is almost no difference in the extent of uptake of the three REEs. At high REE concentration, a fractionation in the extent of uptake seems to occur, with the uptake percentage following the order Yb(III) ≥ Eu(III) > La(III), in particular, when Al-nZVI or alumina are used. This issue is discussed in more details in next section.

The pH of REEs solutions was measured at the end of the uptake process. The final pH values are provided in Tables 3 and 4 for the initial REE concentrations of 1.0 mg L^{-1} and 100 mg L^{-1}. As mentioned in Section 3.1, the zpc of nZVI is 8.3. Hence, based on the final pH values, the surface of nZVI is expected to be negatively charged enabling the uptake to occur through attachment of REEs to the exposed FeO^- and $FeOO^-$ groups on the external nZVI surface. In the case of Al-nZVI, the measured final pH values are smaller than those measured for pure nZVI. However, since Al-nZVI is a heterogeneous material, the pH of the bulk solution does not reflect the difference in the surface charge of iron and aluminum oxides in the composite material. Iron oxides/oxyhydroxides are more basic than aluminum oxide, and as such the uptake of REEs on this composite material is expected to be dominated by its nZVI content as a result of its higher basicity and high surface area resulting from its nano-dimension. Further comments on the uptake mechanism are given in Section 3.3.

In all the experiments, it is noticed that the uptake is smallest at pH of 1.0. Among other factors pertaining to speciation of metals

Table 3
Final pH values measured for REEs initial concentrations of 1.0 mg L^{-1}.

Initial pH	Equilibrium pH		
	Al-nZVI	nZVI	Al_2O_3
1.0	2.90	2.88	1.09
2.0	2.76	7.88	2.40
3.0	3.78	8.74	3.45
4.0	3.86	8.79	3.81
5.0	6.09	8.61	3.34
6.0	6.37	8.40	3.39
7.0	6.96	8.50	3.41
8.0	8.03	8.80	3.31

and competitive behavior of H^+, the lower uptake at this pH could be caused mainly by partial dissolution of the iron materials, as the concentration of iron in solution at the end of uptake was 1556 mg L^{-1}. Taking into consideration that 100 mg nZVI or Al-nZVI was used in 10 mL REEs solution aliquots, the amount of dissolved iron corresponds to about 15% of the total mass of nZVI used, and roughly 30% of iron mass in Al-nZVI. At subsequent pH values, the amount of dissolved iron was observed to decrease largely, varying between 60 and 160 mg L^{-1}, i.e. less than 1.6% of the initial nZVI amount. In light of these results and since the low pH could lead to dissolution of iron while high pHs may result in hydrolysis of REEs, the subsequent experiments were carried out at pH 5.0.

3.2.2. Effect of shaking time on uptake of REEs

In each of these experiments, 100 mg of nZVI or Al-nZVI was mixed with 10.0 mL of two different initial concentrations, i.e. 10.0 mg L^{-1} and 100.0 mg L^{-1} of REEs, at solution pH of 5.0. The samples were shaken for 5 min, 10 min, 30 min, 1 h, 4 h and 24 h. The results show that the uptake of REEs on nZVI has very fast kinetics. Even at the initial concentration of 100.0 mg L^{-1}, REEs appeared to be removed almost completely (%uptake > 99) within the first 5 min of contact with nZVI. The same behavior is also observed for Al-nZVI when the initial REEs concentration is 10.0 mg L^{-1}. However, when the concentration of REEs is increased to 100.0 mg L^{-1}, equilibrium seems to be approached at later times and the uptake is far from being complete specially for La(III), as seen in Fig. 5. The decrease in uptake at longer times might be explained by certain extent of desorption of ions that are weakly bonded to the substrate surface during the earlier times of contact. Nevertheless, it is noticed that the uptake of Eu(III) and Yb(III) is still higher than 50% in the first 5 min of contact. Based on this a period of 30 min of shaking time was chosen to be applied in the next experiments.

Comparing the behavior of nZVI and Al-nZVI it can be seen that the former is more effective in terms of the speed as well as the extent of uptake of REEs. A faster uptake indicates a smaller barrier against uptake of REEs in the case of nZVI, which can be linked to easier accessibility imparted by the nanosize of the material. The higher extent of uptake, considered in the previous section, can be related mainly to the negative surface charge being more dominant in the case of nZVI compared with Al-nZVI. This is confirmed by the

Table 4
Final pH values measured for REEs initial concentrations of 100.0 mg L^{-1}.

Initial pH	Equilibrium pH		
	Al-nZVI	nZVI	Al_2O_3
1	4.77	3.43	1.47
3	4.00	8.53	4.19
4	4.76	8.68	4.58
5	5.64	8.55	3.16
6	6.35	8.60	3.22

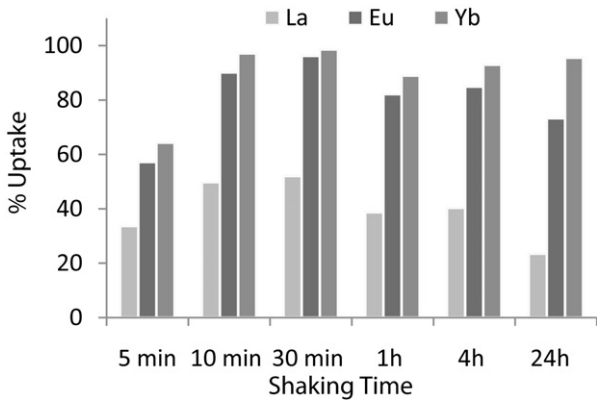

Fig. 5. La(III), Eu(III), and Yb(III) uptake on Al-nZVI as a function of shaking time. C_i: 100.0 mg L^{-1}; m: 100 mg; V: 10 mL; pH: 5.0.

equilibrium pH values which were found to be 8.6 in the case of nZVI and 6.1 in the case of Al-nZVI.

The fractionation behavior reported in the previous section appears to be clear in Fig. 5, with the extent of uptake following the order: Yb(III) > Eu(III) > La(III). Fractionation of REEs was reported earlier for sorption on clay minerals [18], with LREEs being sorbed to lesser extent than HREEs. The behavior was attributed to the decrease in ionic radius with the increasing atomic number. Moreover, it was reported that the fractionation becomes distinct at higher ionic strength [18]. The fractionation behavior could be linked to another factor; the change in coordination number of REEs in their aqueous complexes. It has been suggested that the hydration number of the REE aquo-ions changes from 9 for the light REE (LREE) to 8 for the heavy REE (HREE) with a transition region from Sm to Gd [19]. Higher coordination number is expected to restrict the bulk diffusion of an ion in its way toward the sorption site. On the contrary, opposite fractionation trends were observed for sorption of REEs from seawater onto iron and manganese oxides [20]. The behavior was attributed to the formation of more stable inorganic complexes in sea water by HREEs, and was shown to depend also on the crystallinity and particle size of the sorbent phase.

3.2.3. Effect of initial metal concentration on uptake of REEs

The effect of initial REEs concentrations on the extent of uptake is shown in Fig. 6. The figure contains only the results for La(III) since other REEs showed similar trends. In general, the uptake of REEs on nZVI was above 99% over the entire range of concentrations. If pure

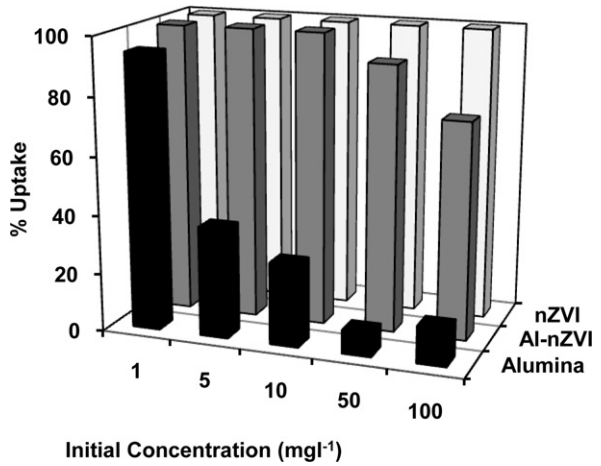

Fig. 6. Effect of initial metal concentration on the uptake of La(III) ion on nZVI, Al-nZVI and Al_2O_3 (m: 100 mg; V: 10 mL; shaking time: 30 min; pH: 5.0).

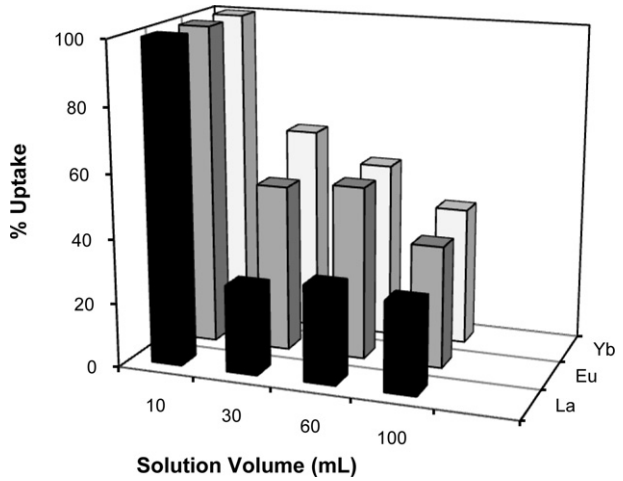

Fig. 7. The effect of solution volume on the uptake of La(III), Eu(III), and Yb(III) on Al-nZVI (C_i: 50.0 mg L^{-1}; m: 100 mg; pH: 5.0).

alumina is used, the uptake percentage is seen to drop dramatically as the initial concentration of REEs is increased. The association of nZVI with alumina can be seen as a means by which the uptake performance of the mineral can be significantly enhanced, as suggested by the results in Fig. 6.

To further assess the uptake performance of Al-nZVI, the effect of solution volume on the extent of sorption was also investigated. For this purpose, 100 mg samples of Al-nZVI were separately added to 10, 30, 60 and 100 mL of REEs solution at pH of 5.0 and initial REEs concentration of 50.0 mg L^{-1}. Increasing the solution volume helps dilute the concentration of the sorbent material, providing for better dispersion of it in the solution and thus enhances its exposure to the REE ions. From another side, for a given constant concentration, increasing the solution volume increases the number of REE ions available in solution. The obtained results are shown in Fig. 7. As can be seen from the figure, a solution volume of 10.0 mL of 50.0 mg L^{-1} REEs provided the best results. As the solution volume increases, it seems that the effect of increasing REE ion concentration largely surpasses the effect of the presumably increasing dispersion of the Al-nZVI material. This might be indicative that the nZVI component in Al-nZVI is not liable to dispersion in the solution body, i.e. that it is somehow tightly connected to the composite matrix.

Table 5
Standard cell potentials for various La, Eu, and Yb ions.

Reaction	E° (V)
Acidic solution	
$La^{3+} \rightarrow La$	−2.38
$Eu^{3+} \rightarrow Eu^{2+}$	−0.35
$Eu^{2+} \rightarrow Eu$	−2.80
$Eu^{3+} \rightarrow Eu$	−1.99
$Yb^{3+} \rightarrow Yb^{2+}$	−1.05
$Yb^{2+} \rightarrow Yb$	−2.80
$Yb^{3+} \rightarrow Yb$	−2.22
Basic solution	
$La(OH)_3 \rightarrow La$	−2.80
$Eu(OH)_3 \rightarrow Eu$	−2.51
$Yb(OH)_3 \rightarrow Yb$	−2.74

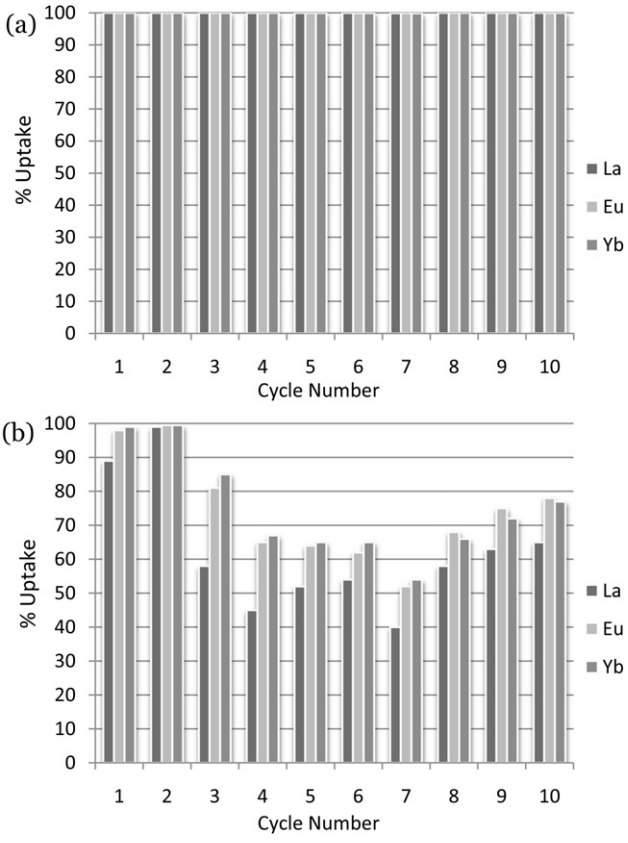

Fig. 8. Percentage uptake of La(III), Eu(III), and Yb(III) as a function of reusability of nZVI. (a) C_i: 1.0 mg L^{-1}; m: 100 mg; V: 10 mL; pH: 5.0 and (b) C_i: 50.0 mg L^{-1}; m: 100 mg; V: 10 mL; pH: 5.0.

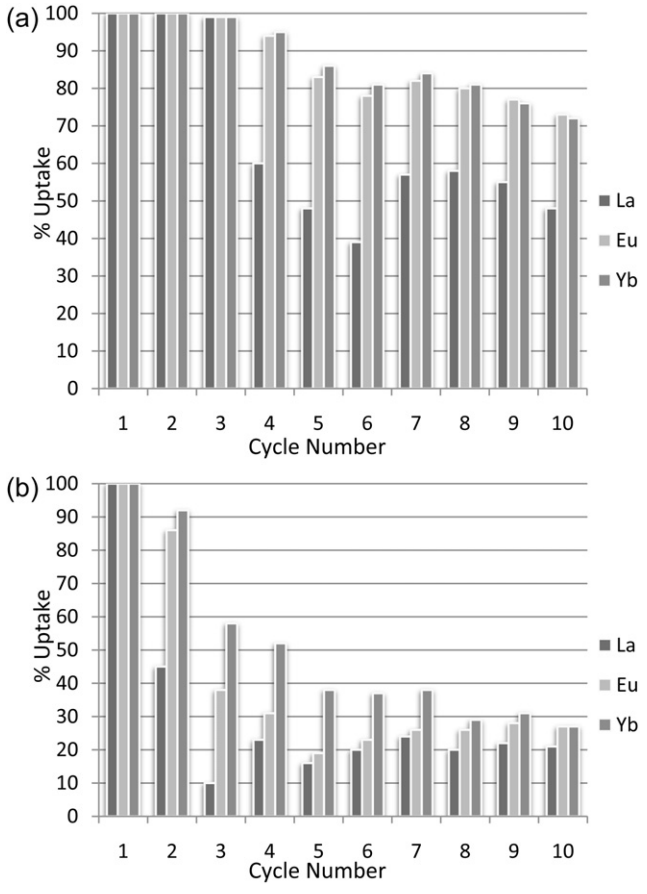

Fig. 9. Percentage uptake of La(III), Eu(III), and Yb(III) as a function of reusability of Al-nZVI. (a) C_i: 1.0 mg L^{-1}; m: 100 mg; V: 10 mL; pH: 5.0. (b) C_i: 50.0 mg L^{-1}; m: 100 mg; V: 10 mL; pH: 5.0.

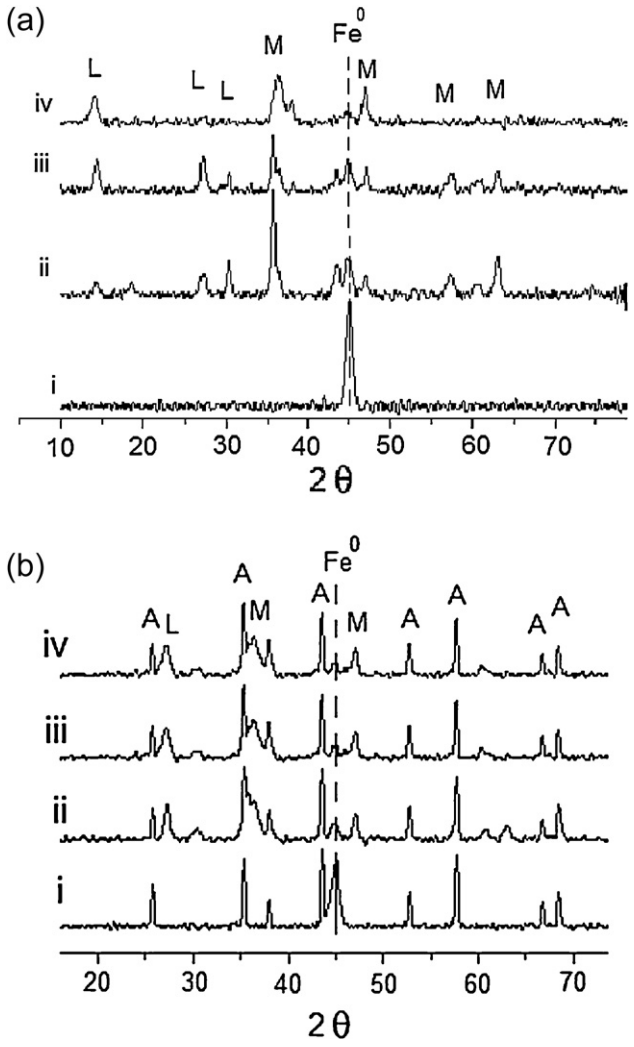

Fig. 10. XRD patterns of (a) nZVI samples and (b) Al-nZVI samples: (i) pure nZVI or Al-nZVI, (ii) nZVI or Al-nZVI after shaking with water, (iii) nZVI or Al-nZVI after contact with 10 mg L^{-1} REEs, and (iv) nZVI or Al-nZVI after contact with 50 mg L^{-1} REEs. A: alumina (Al_2O_3); Fe^0: nZVI; M: magnetite/maghemite (Fe_3O_4/γ-Fe_2O_3); L: lepidocrocite (γ-FeOOH).

3.2.4. Repetitive reactivity tests

The reusability of the nZVI and Al-nZVI samples was also investigated at two initial REE concentrations of 1.0 mg L^{-1} and 50 mg L^{-1}. In these experiments, the REE solutions were exposed to the same samples of nZVI and Al-nZVI for ten successive cycles of uptake. The results are shown in Fig. 8 for nZVI and in Fig. 9 for Al-nZVI. Fig. 8 indicates that nZVI can be reused 10 times with a high sorption capacity toward REEs at both REEs concentrations. According to Fig. 9, Al-nZVI can also be reused 10 times with a high sorption capacity toward REEs at the initial concentration of 1.0 mg L^{-1}, but in the case of 50 mg L^{-1}, the uptake capacity of Al-nZVI deteriorates after two cycles of reusability.

The results of the above experiments form another clue of the effectiveness of nZVI toward fixation of REEs. The observed behavior might be related to the uptake mechanism of REEs which is discussed in the next section.

3.3. Comments on the uptake mechanism of REEs

As was shown in earlier investigations, some of which reported by our group [e.g. 11,17,21], nZVI is well known to possess a core-shell structure. This structure enables the material to demonstrate basically two uptake mechanisms toward metallic ions. The core, composed of zero-valent iron, forms an electron source that might reduce ions possessing higher standard reduction potentials than iron. The shell, on the other hand, possesses hydroxyl and oxide groups at the interface with the solution and is capable, as a result, to fix adsorbate ions by surface complexation. The possibility of surface precipitation cannot be ruled out at higher ion concentration in high pH media.

REEs are known to possess standard electrode potentials (Table 5), [22], well below that of iron (−0.41 V). Hence, in the absence of a driving force for redox reactions, the uptake of REEs by iron nanoparticles is expected to occur on the external surface of the shell of nanoparticles. In our previous investigations using HR-TEM, SAED, and XPS [11,17,21], the shell was found to be less than 5 nm thick, amorphous, and contains oxide and oxyhydroxide groups at its external surface. In solution, the oxidation of iron nanoparticles increases the density of surface sites available for interaction with REE ions. Nevertheless, the oxidation may result in aggregation of the nanoparticles and thus dramatically reduce the surface area of the adsorbent, consequently decreasing the extent of surface uptake. As shown in Fig. 10, XRD investigation showed massive development of iron oxide and oxyhydroxide during the uptake process on nZVI and Al-nZVI. The oxidation is reflected also by the HR-TEM images shown in Fig. 11 for nZVI and Al-nZVI following the uptake of REEs. TEM images of Al-nZVI showed aggregation of originally dispersed nZVI nano-crystals accompanied with intensive formation of needle-like structure with a length that amounts to several hundred nanometers occasionally. The width of the needles appears in the range 5–20 nm. The oxidation of iron nanoparticles seemed to be associated also with loss of lattice fringes indicating the amorphous nature of the oxide layers.

In general, the uptake mechanism of REEs is not an easy issue to tackle. These metals possess rich solution chemistry due to their liability to complexation by various types of ligands. It has been reported that in the presence of OH^- ligands, for example, a variety of lanthanide species might form. These include $Ln(OH)_2^+$, $Ln(OH)_3^0$, $Ln(OH)_4^-$, $Ln(OH)_5^{2-}$, $Ln(OH)_6^{3-}$, in addition to polymeric species [19]. In this study, the major anions in solution are OH^- and Cl^-, the latter originating from iron chloride salt used in the preparation of iron nanoparticles. It is documented that REE complexes with Cl^- are relatively weak outer sphere complexes [19,23,24]. Consequently the speciation of REEs will be dominated by their hydroxyl species.

Minerals can take up REEs from aqueous solutions through a variety of scavenging processes including adsorption, formation of surface solid solutions, and surface precipitation [25]. Unless the hydroxide concentration is high, the dominant oxidation state of REEs in aqueous solution at 25 °C is the +3 state [19]. This high oxidation state makes REEs behave as hard acids that can bind strongly to oxide and oxyoxide groups. As a first approximation, under proper pH conditions, the surface reaction on *mononuclear* oxide and oxyoxide sites with the bare REE ions can be represented by:

$$M^{3+} + FeOO^- \rightarrow FeOOM^{2+}$$

$$M^{3+} + FeO^- \rightarrow FeOM^{2+}$$

M^{3+} stands for REE ions. The bonds of REEs in such complexes are expected to possess mainly electrostatic rather than covalent character. These reactions might be extended to include the other cationic forms of REEs, $M(OH)_2^+$, yielding the hydrolyzed REE species $FeOOM(OH)_2$ and $FeOM(OH)_2$.

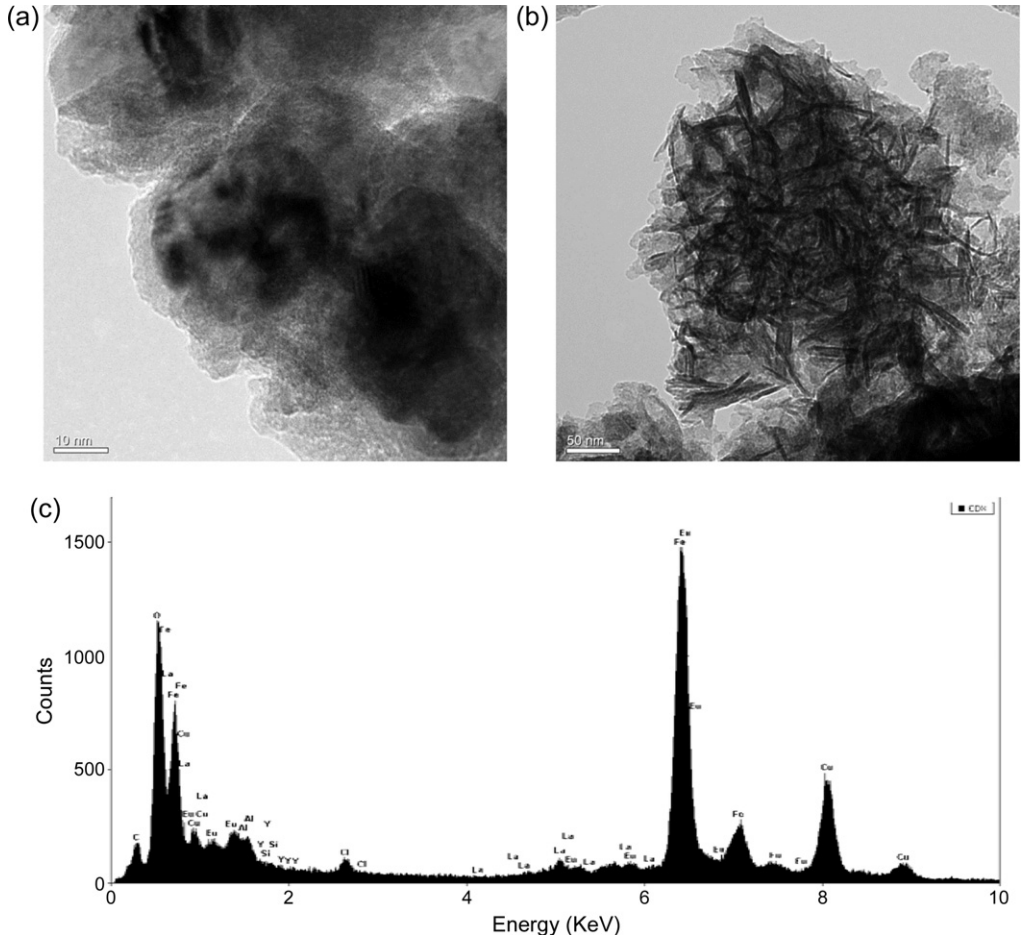

Fig. 11. (a and b) HR-TEM images showing partial and massive oxidation of iron nanoparticles after contact with REEs, (c) EDX spectrum of Al-nZVI after contact with REEs.

In addition, the uptake of REEs on oxide surfaces was also suggested to take place on *heteronuclear* surface sites [25]. Such reactions can yield a variety of surface species depending on the operating conditions, nature of surface, and REE chemical form [25,26]. In this case, two charged and two neutral sites per adsorbed metal are suggested to be involved. Examples of the outcome of such uptake include $(\rangle SOH)_2(\rangle SO^-)_2\_M^{3+}$, $(\rangle SOH)_2(\rangle SO^-)_2\_M(OH)^{2+}$, $(\rangle SOH)_2(\rangle SO^-)_2\_M(OH)_2^+$, $(\rangle SOH)_2(\rangle SO^-)_2\_M(OH)_3$ [25], where S stands for the surface site and M for the metal. Apart from these complexation reactions, in particular at high pH values, surface precipitation of $M(OH)_{3(s)}$ could also be possible.

Finally, the comments above do not take into consideration the impact of individual differences among various REEs on the uptake mechanism. Charge density is known as an important factor in determining the liability of cations to complexation and the extent of their uptake. As mentioned earlier, the fractionation of uptake of REEs becomes more distinct at higher loadings. Our previous investigations on a group of metallic ions [11] indicated that at high concentrations, the charge density of the cation becomes increasingly effective in determining its extent of uptake on nZVI. This could be explained by the relatively higher ability of smaller cations at the right edge of lanthanides to diffuse from outer-sphere coordination into inner-sphere environment in which cations could bind to inner oxygen atoms in oxyhydroxyl/oxide groups in the shell of nanoparticles.

4. Conclusions

nZVI is an effective material for the removal of REEs from aqueous solutions. The material demonstrated outstanding uptake ability over a wide range of experimental conditions, and appeared to continue to be effective in multiple cycles of usage. Incorporation of nZVI on alumina enhances the removal capacity of the mineral by several folds. REEs demonstrated fractionation on Al-nZVI, with the LREEs being less sorbed compared with HREEs. The mechanism of uptake is suggested to proceed via surface precipitation and/or complexation of REEs with surface groups containing oxide and oxyhydroxide groups of iron.

Acknowledgements

The authors thank Dr. Ingo Lieberwirth at Max Planck Institute for Polymer Research, Germany for his help in HR-TEM analysis. The authors are grateful to the Center of Materials Research at İzmir Institute of Technology for the help in XRD, SEM/EDX and BET-N_2 analysis.

References

[1] Z. Chen, Journal of Rare Earths 29 (2011) 1–6.
[2] http://pubs.usgs.gov/sir/2011/5094/pdf/sir2011-5094.pdf (accessed 26.09.12).
[3] P. Liang, Y. Liu, L. Guo, Spectrochimica Acta Part B 60 (2005) 125–129.
[4] F. Fujimori, T. Hayashi, K. Inagaki, H. Haraguchi, Fresenius Journal of Analytical Chemistry 363 (1999) 277–282.
[5] M.B. Shabani, T. Akagi, H. Shimizu, A. Masuda, Analytical Chemistry 62 (1990) 2709–2714.
[6] T.H. Zhang, X.Q. Shan, R.X. Liu, H.X. Tang, S.Z. Zhang, Analytical Chemistry 70 (1998) 3964–3968.
[7] P. Moller, P. Dulski, J. Luck, Spectrochimica Acta Part B 47 (1992) 1379–1387.
[8] T. Pasinli, A.E. Eroğlu, T. Shahwan, Analytica Chimica Acta 547 (2005) 42–49.
[9] Y. Andrès, A.C. Texier, P. Le Cloirec, Environmental Technology 24 (2003) 1367–1375.

[10] W. Yan, A.A. Herzing, C.J. Kiely, W-X. Zhang, Journal of Contaminant Hydrology 118 (2010) 96–104.
[11] N. Efecan, T. Shahwan, A.E. Eroğlu, I. Lieberwirth, Desalination 249 (2009) 1048–1054.
[12] K.-H. Shin, D.K. Cha, Chemosphere 72 (2008) 257–262.
[13] Y.P. Katsenovich, F.R. Miralles-Wilhelm, Science of the Total Environment 407 (2009) 4986–4993.
[14] T. Shahwan, S. Abu Sirriah, M. Nairat, E. Boyaci, A.E. Eroglu, T.B. Scott, K.R. Hallam, Journal of Chemical Engineering 172 (2011) 258–266.
[15] Y. An, T. Li, Z. Jin, M. Dong, H. Xia, X. Wang, Bioresource Technology 101 (2010) 9825–9828.
[16] http://www.who.int/water_sanitation_health/dwq/chemicals/iron.pdf (accessed 25.09.12).
[17] D. Karabelli, S. Unal, T. Shahwan, A.E. Eroglu, Journal of Chemical Engineering 168 (2011) 979–984.
[18] F. Coppin, G. Berger, A. Bauer, S. Castet, M. Loubet, Chemical Geology 182 (2002) 57–68.
[19] S.A. Wood, Chemical Geology 82 (1990) 159–186.
[20] D. Koeppenkastrop, E.H. De Carlo, Chemical Geology 95 (1992) 251–263.
[21] Ç. Üzüm, T. Shahwan, A.E. Eroğlu, K.R. Hallam, T.B. Scott, I. Lieberwirth, Applied Clay Science 43 (2009) 172–181.
[22] http://www.webelements.com (accessed 25.09.12).
[23] H.B. Silber, Inorganica Chimica Acta 139 (1987) 33–38.
[24] G. Johansson, H. Wakita, Inorganic Chemistry 24 (1985) 3047–3052.
[25] W. Piasecki, D.A. Sverjensky, Geochimica et Cosmochimica Acta 72 (2008) 3964–3979.
[26] K.A. Quinn, R.H. Byrne, J. Schijf, Aquatic Geochemistry 10 (2004) 59–80.